Acta Biochim Biophys Sin 2011, 43: 172–180 | © The Author 2011. Published by ABBS Editorial Office in association with Oxford University Press on behalf of the Institute of Biochemistry and Cell Biology, Shanghai Institutes for Biological Sciences, Chinese Academy of Sciences. DOI: 10.1093/abbs/gmr002.
Advance Access Publication 2 February 2011

Original Article

Structural and thermodynamics characters of isolated α-syn12 peptide: long-time temperature replica-exchange molecular dynamics in aqueous solution

Zanxia Cao[1,2], Lei Liu[1,3], Ping Wu[4], and Jihua Wang[1,2*]

[1]Key Lab of Biophysics in Universities of Shandong, Dezhou 253023, China
[2]Department of Physics, Dezhou University, Dezhou 253023, China
[3]Department of Computer Science and Technology, Dezhou University, Dezhou 253023, China
[4]Department of Chemistry, Dezhou University, Dezhou 253023, China
*Correspondence address. Tel: +86-534-8985933; Fax: +86-534-8985884; E-mail: jhwyh@yahoo.com.cn

The structural and thermodynamics characters of α-syn12 (residues 1–12 of the human α-synuclein protein) peptide in aqueous solution were investigated through temperature replica-exchange molecular dynamics (T-REMD) simulations with the GROMOS 43A1 force field. The two independent T-REMD simulations were completed starting from an initial conformational α-helix and an irregular structure, respectively. Each replica was run for 300 ns. The structural and thermodynamics characters were studied based on parameters such as distributions of backbone dihedral angles, free energy surface, stability of folded β-hairpin structure, and favorite conformations. The results showed that the isolated α-syn12 peptide in water adopted four different conformational states: the first state was a β-hairpin ensemble with $Turn_{9-6}$ and four hydrogen bonds, the second state was a β-hairpin ensemble with two turns ($Turn_{9-6}$ and $Turn_{5-2}$) and three hydrogen bonds, the third state was a disordered structure with both $Turn_{8-5}$ and $Turn_{5-2}$, and the last state was a π-helix ensemble. Meanwhile, we studied the free energy change of α-syn12 peptide from the unfolded state to the β-hairpin state, which was in good agreement with the experiments and molecular dynamics simulations for some other peptides. We also analyzed the driving force of the peptide transition. The results indicated that the driving forces were high solvent exposure of hydrophobic Leu8 and hydrophobic residues in secondary structure. To our knowledge, this was the first report to study the isolated α-syn12 peptide in water by T-REMD.

Keywords α-syn12; temperature replica exchange; molecular dynamics simulation; free energy surface

Received: July 25, 2010 Accepted: November 18, 2010

Introduction

Extensive evidence has been accumulated in recent years on the fact that several protein conformational diseases have the same molecular basis: conformational change from a prevailing α-helical structure to a β-sheet-rich structure. These diseases include Alzheimer's disease, prion-related disorders, Parkinson's disease, etc. [1–6]. Alzheimer's disease is the result of aberrant deposition of amyloid-beta in the form of a β-sheet in the brain [7–9]. The pathology of prion-related disorders includes the accumulation of prion protein [10,11]. Parkinson's disease is characterized by the deposition of aggregated fibrillar α-synuclein in Lewy bodies (LBs) within the brain [12–18].

Human α-synuclein protein, a presynaptic protein of 140 amino acid residues, which usually has extensive intrinsically disordered regions, is the major component of LBs deposited in the brains of patients with Parkinson's disease. Typical of Parkinson's disease is the presence of α-synuclein aggregates in the form of a β-structure that can be soluble or insoluble [17]. The structure (PDB (Protein Data Bank) ID: 1xq8) of micelle-bound human α-synuclein has been studied by Ulmer *et al*. [18] with solution NMR spectroscopy. Val3–Val37 and Lys45–Thr92 in α-synuclein form curved α-helices with a break in the 38–44 regions. On the contrary, an uninterrupted helix has been proposed from site-directed spin labeling–electron paramagnetic resonance experiments in the presence of small unilamellar vesicles [19].

Synphilin-1 is a novel α-synuclein interacting protein presenting in LBs [20]. Xie *et al*. [21] reported that the N-terminal 12-residue peptide of α-synuclein (α-syn12) could effectively compete with the N-terminal 65-residue peptide of α-synuclein for binding to the coiled-coil domain of synphilin-1. Unfortunately, so far the structure of the isolated α-syn12 peptide in water has not been

determined by experimental methods, so that the possible structure of this fragment has not been available.

In this case, one choice is to study the isolated α-syn12 peptide in water by molecular dynamics (MD) simulations. In fact, some researchers have studied other amyloid peptides by MD simulations. For example, Daidone *et al*. [22–24] and Chiang *et al*. [25] studied the folding and α-to-β conformational transition of the Syrian hamster PrP peptide H1 and of the Aβ (12–28) fragment. Levy *et al*. [26] observed the helix-to-coil conformational transition of the PrP (106–126) peptide by performing a set of 34 MD simulations. Klimov and Thirumalai [27] showed that the oligomerization of Aβ (16–22) requires the peptide to undergo a random coil to α-helix to β transition via MD simulations. Cao and Wang [28] investigated the dynamics and thermodynamics characters of H1 peptide (residues 109–122 of the Syrian hamster PrP) in aqueous solution, and the calculated folded free energy from GROMOS 43A1 was comparable with experimental values and other MD simulation results. However, to our knowledge, there has not been any report to study the isolated α-syn12 peptide in water by MD simulations.

There are two factors for the qualities of protein modeling: one is the accuracy of empirical force fields and the other is the efficiency of the sampling method. One advance in solving the sampling problem is the development of the replica-exchange MD (REMD) method [29–33]. Compared with regular MD that only samples a conventional canonical ensemble, REMD can sample a generalized ensemble. REMD simulations are more than four times efficient than multiple independent MD simulations at one temperature [34]. REMD simulations are usually employed to construct free energy surfaces in reduced dimensions [30,35–39].

In this work, we studied the structural and thermodynamics characters of the isolated α-syn12 peptide in explicit water at atomic resolution by long-timescale temperature REMD (T-REMD). Moreover, the driving force in the conformational transition of α-syn12 peptide was analyzed. The two independent T-REMD simulations were completed starting from different initial conformations of an α-helix (from PDB ID: 1xq8) and an irregular structure (from PDB ID: 2JN5), respectively. Each replica was run for 300 ns, and the total MD simulation time was 10.8 μs. The last 100 ns of trajectory at 300 K was analyzed. The structural and thermodynamics characters were analyzed from parameters such as distributions of backbone dihedral angles, free energy surface, stability of folded β-hairpin structure, and favorite conformations.

Materials and Methods

The α-syn12 peptide (residues 1–12 of the human α-synuclein protein; the sequence is MDVFMKGLSKAK) was chosen for study. MD simulation in the isothermal–isobaric (NPT) ensemble was performed using the GROMACS software package [40] with the GROMOS 43A1 [41] force field. The peptide was solvated in a rectangular box of the single point charge (SPC) water model [42] with the minimum solute-box boundary distance set to 1.4 nm. Protonation states of ionizable groups were chosen for pH 7.0.

In the explicit-solvent simulations, the non-bonded interactions were treated using a twin-range cutoff method [43] with generalized reaction field corrections, in which short-range interactions within 0.8 nm were evaluated every step, medium-range interactions between 0.8 and 1.4 nm were updated every 10 steps, and electrostatic interactions beyond 1.4 nm were approximated by reaction fields generated by a dielectric continuum with a dielectric constant of 54 for water. The temperature and pressure of the system were kept constant by weak coupling to external heat baths with a relaxation time of 0.1 ps [44]. The time step for the MD integrator was set to 2 fs and SHAKE [45] was applied to constrain all bond lengths with a relative tolerance of 10^{-4}.

Thirty-two replicas were simulated at temperatures (in K) of 273, 276, 279, 281, 284, 287, 290, 293, 296, 299, 302, 305, 309, 312, 315, 318, 321, 324, 328, 331, 334, 338, 341, 345, 348, 351, 355, 358, 362, 365, 369, and 373 [46]. The two independent T-REMD simulations were performed starting from an α-helix (from PDB ID: 1xq8, noted as simulation 1) and an irregular structure (from PDB ID: 2JN5, noted as simulation 2), respectively. Each replica was equilibrated at its respective temperature for 100 ps. A total of 300 ns T-REMD simulations were performed for each replica. The replica exchanges were attempted every 2 ps based on the Metropolis criterion. Coordinates and energies were recorded every 2 ps. The trajectory of 300 K was evenly divided into three 100 ns blocks, noted as the first block, the second block, and the last block. It should be noted that the convergence of conformation sampling starting from the α-helix was verified by the simulations starting from an irregular structure.

Results

T-REMD simulations

Effective T-REMD requires sufficient exchange between the different temperatures (the ratio of exchange is >0.1). The ratios of successful exchange attempts were between 22% and 40% in these simulations, so the number of replicas was sufficient.

Backbone dihedral angle distributions of the α-syn12 peptide

We analyzed the distributions of the backbone (ϕ, ψ) angles for residues 2–11. The data for these residues were pooled together. The distributions of the dihedral (ϕ, ψ)

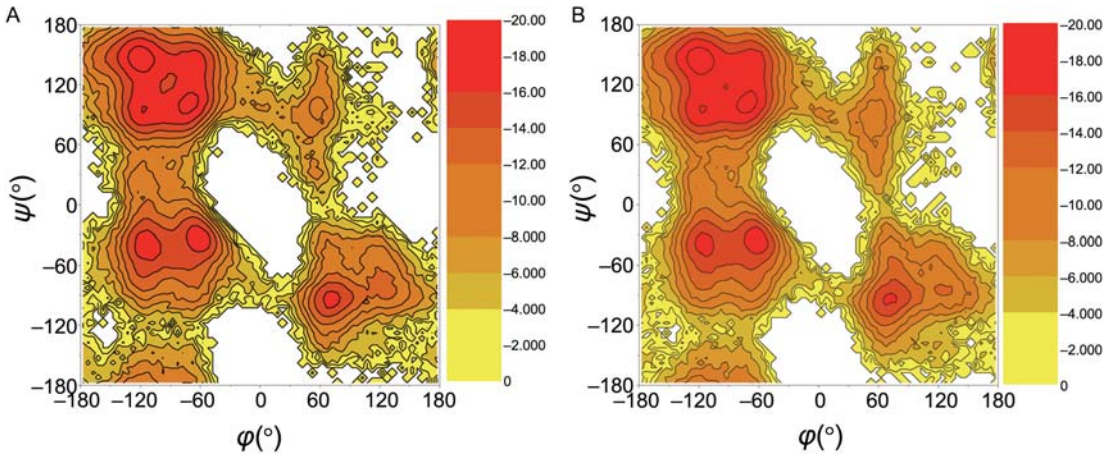

Figure 1 Potential of mean forces obtained from (ϕ, ψ) distributions for residues 2–11 (A) Simulation starting from the α-helix for the last 100 ns trajectory. (B) Simulation starting from the irregular structure for the last 100 ns trajectory. The red regions correspond to the lowest energy areas. Neighboring contour lines are separated by 2 kJ mole^{-1}.

Table 1 Respective probabilities for (ϕ, ψ) angles falling into different regions from different simulations and different time blocks

	α-Region			β-Region		
	From block 1	From block 2	From block 3	From block 1	From block 2	From block 3
From α-helix	0.32	0.26	0.23	0.49	0.55	0.56
From irregular	0.27	0.19	0.21	0.52	0.60	0.58

angles of each residue were collected from the simulations, and potentials of mean force were computed (**Fig. 1**).

The total 300 ns trajectory set of 300 K was evenly divided into three 100 ns blocks for each simulation. The distributions sampled by different simulations and different blocks were in general quite similar to each other. Different regions are defined as in reference [47]: α-region: $-180^\circ < \phi < 0^\circ$ and $-120^\circ < \psi < 30^\circ$; bridge region: $-180^\circ < \phi < 0^\circ$ and $30^\circ < \psi < 90^\circ$; β-region: $-180^\circ < \phi < 0^\circ$, and $90^\circ < \psi < 180^\circ$ or $-180^\circ < \psi < -120^\circ$. For the first simulation, the probabilities for (ϕ, ψ) angles to fall into the α-region were 32%, 26%, and 23% in the first block, second block, and third block, respectively; the respective probabilities for (ϕ, ψ) angles to fall into the β-region were 49%, 55%, and 56%. For the second simulation, the probabilities for (ϕ, ψ) angles to fall into the α-region were 27%, 19%, and 21% in the first block, second block, and third block, respectively; the respective probabilities for (ϕ, ψ) angles to fall into the β-region were 52%, 60%, and 58% (**Table 1**).

The convergence of the conformational sampling in the first simulation was verified by the second simulation starting from an irregular structure. To evaluate the convergence of the conformational sampling of the simulations, one way is based on the distribution probabilities of dihedral angles (ϕ, ψ) to fall into different regions as a function of time. The simulation starting from an α-helix structure produced more sampling in the α-region relative to the second simulation starting from an irregular structure in the first and second time blocks. But in the third time block, the simulation starting from an α-helix structure produced almost the same sampling in the α-and β-region as those starting from an irregular structure (**Table 1**), which indicated that the last 100 ns was convergent. So in this work, we only used the last 100 ns of the trajectory at 300 K to study the peptide. Although the method used to estimate the convergence of conformational sampling was crude, the free energy surface calculations further showed that it was indeed convergent for simulations starting from different conformations in the latter part of this paper.

Figure 1 showed that there was some sampling in the α-region in the two independent simulations. It is interesting to know whether significant helical content (including α-helix, π-helix, and 3_{10}-helix) was found in the simulations. The helical content calculated by the program STRIDE [48,49] was 7%–8% for both the simulations. The simulations produced more sampling in the β-region than in the α-region. The experiments indicated that the β-sheet structure was enhanced and a significant amount of α-helical secondary structure was retained during the formation of α-synuclein oligomers under physiological conditions or in methanol–water solutions [50]. The above simulation results were consistent with the experiments.

Free energy surface of the α-syn12 peptide

The free energy surfaces were constructed using two principal components (PC1 and PC2) as the reaction coordinates (**Fig. 2**). The programs 'g_covar' and 'g_anaeig' in the GROMACS package were used in the principal components

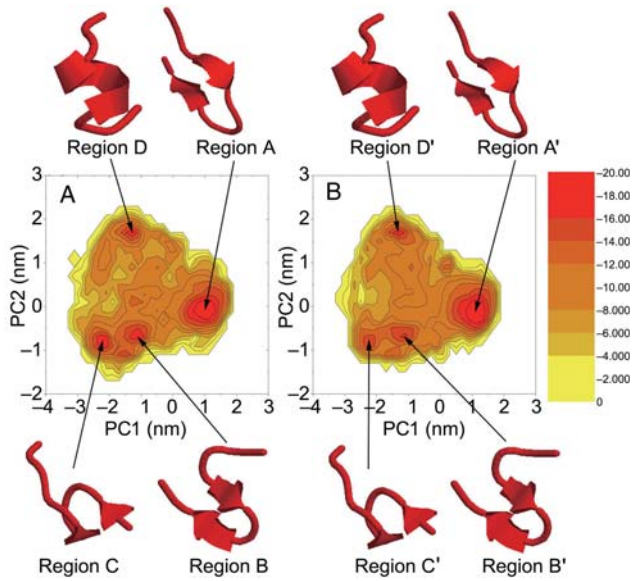

Figure 2 Free energy surfaces projected to the first two principal components (PC1 and PC2) (A) Simulation starting from the α-helix for the last 100 ns trajectory. (B) Simulation starting from the irregular structure for the last 100 ns trajectory. The red regions correspond to the lowest energy areas. Neighboring contour lines are separated by 2 kJ mole^{-1}. Representative structures of the four highly populated regions are shown.

analysis (PCA) [51]. This set of principal components was used as reaction coordinates to describe free energy surfaces at 300 K. In PCA, only fluctuations of all the backbone atoms of this peptide (93 atoms) were used. Here we chose the first two principal components (PC1 and PC2) as the reaction coordinates (**Fig. 2**). For these two simulations at 300 K, there were four highly populated regions on the PCA map centered near (1.0, 0.0 nm), (−1.0, −0.7 nm), (−2.2, −0.8 nm), and (−1.3, 1.7 nm). $Turn_{9-6}$ denotes a β-turn forming among residues 6–9. HB_{4-11} is defined as hydrogen bond between the hydrogen atom of the amide NH of residue 4 and the backbone carbonyl oxygen atom of residue 11. The formation of β-turn and hydrogen bond was estimated by the program STRIDE. The corresponding representative structures are shown in **Fig. 2**. We obtained the local minima in the four regions: (A) located at (1.0, 0.0 nm) of (PC1, PC2), which corresponds to the β-hairpin ensemble with $Turn_{9-6}$ and four hydrogen bonds (HB_{4-11}, HB_{6-9}, HB_{9-6}, and HB_{11-4}); (B) located at (−1.0, −0.7 nm), corresponding to a β-hairpin ensemble with two turns ($Turn_{9-6}$ and $Turn_{5-2}$) and three hydrogen bonds (HB_{6-9}, HB_{9-6}, and HB_{11-4}); (C) located at (−2.2, −0.8 nm), corresponding to a disordered structure with $Turn_{8-5}$ and $Turn_{5-2}$; (D) located at (−1.3, 1.7 nm), corresponding to the π-helix ensemble.

From the first simulation, we obtained the relative depths of the A, B, C, and D minima, which were 0.0, 1.8, 2.8, and 1.6 kJ mole^{-1}; in the second simulation, the corresponding depths were 0.0, 3.2, 5.0, and 1.9 kJ mole^{-1}, respectively. The results indicated that the relative sampling difference mainly appeared in the local minima B and C in the two simulations.

Table 2 Respective probabilities of conformation falling into different clusters for the simulations

	Cluster 1	Cluster 2	Cluster 3	Cluster 4
From α-helix	0.47	0.11	0.15	0.10
From irregular	0.54	0.07	0.07	0.09

Conformation clusters of the α-syn12 peptide

Although the above approach of using two-dimensional reaction coordinates to visually represent the conformational space of peptides was a simple and widely used method, unavoidably, the free energy contour maps depend on the reaction coordinates. Another way to reveal the favorite conformations of the α-syn12 peptide in solution was to cluster them based on their mutual root-mean-square deviations of Ca positions ($RMSD_{Ca}$). For the two independent simulations, we chose to study the conformations of the 300 K replica. A total of 10,000 conformations from the last 100 ns trajectory were clustered based on their pairwise $RMSD_{Ca}$. The criteria of clustering are that the conformations are in the same cluster when $RMSD_{Ca}$ is <0.1 nm among the conformations of this cluster, and vice versa. In addition, all the conformations in the same cluster should be connected by the $RMSD_{Ca}$ criteria. By the clustering criteria, conformations in the simulations fall into clusters of all kinds of sizes. For the first simulation, 195 clusters were obtained. Among them, there were four clusters that contained at least 500 conformations. The representative structure in the first cluster was a β-hairpin with $Turn_{9-6}$ and four hydrogen bonds (HB_{4-11}, HB_{6-9}, HB_{9-6}, and HB_{11-4}). This cluster corresponded to the local minima A in **Fig. 2** and contained 47% of all the conformations. The representative structure in the second cluster was a β-hairpin with two turns ($Turn_{9-6}$ and $Turn_{5-2}$) and three hydrogen bonds (HB_{6-9}, HB_{9-6}, and HB_{11-4}). This cluster corresponded to the local minima B in **Fig. 2** and contained 11% of all the conformations. The representative structure in the third cluster was a disordered structure with both $Turn_{9-6}$ and $Turn_{5-2}$. This cluster corresponded to the local minima C in **Fig. 2** and contained 15% of all the conformations. The representative structure in the fourth cluster was a π-helix. This cluster corresponded to the local minima D in **Fig. 2** and contained 10% of all the conformations.

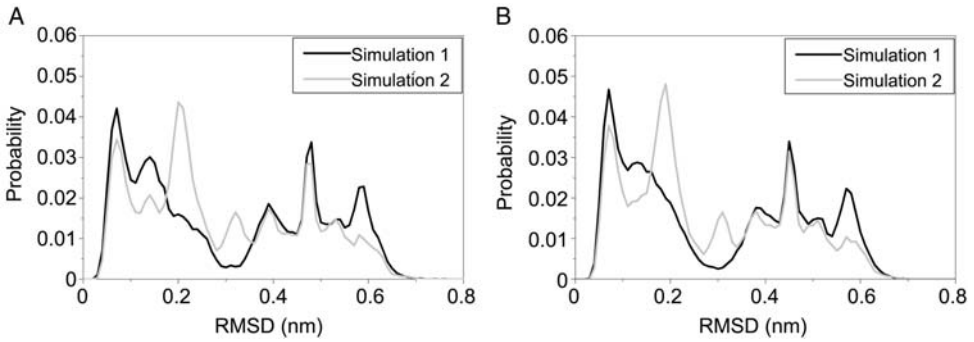

Figure 3 Distributions of the positional RMSDs from representative structure A for the α-syn12 peptide simulated (A) Only the Ca atoms have been considered. (B) All heavy atoms have been considered. The black line corresponds to the simulation starting from the α-helix for the last 100 ns trajectory. The gray line corresponds to the simulation starting from the irregular structure for the last 100 ns trajectory.

For the second simulation, 258 clusters were obtained. Among them, four clusters contained at least 300 conformations. The representative structures of these clusters were the same as the representative structures of clusters in the first simulation. The probabilities of conformation to fall into these clusters were 54%, 7%, 7%, and 9%, respectively (**Table 2**). The β-turn is one of the most important factors in determining the stability of β-hairpins. The numbers of conformation to form Turn_{9-6} were computed in the simulations. The respective probabilities of the conformations having Turn_{9-6} were 76% and 77% for the two simulations. So the β-hairpin configurations can be produced in the simulations for α-syn12 peptide using the GROMOS 43A1 force field, indicating that the α-syn12 peptide in aqueous solution can form a β-sheet.

RMSDs from representative structure A

For peptide simulations, the positional RMSDs of Ca atoms [**Fig. 3(A)**] and all heavy atoms [**Fig.3(B)**] from representative structure A were computed. The distributions of the instantaneous RMSD_{Ca} in the simulations of α-syn12 peptide starting from different conformations were plotted in **Fig. 3(A)**. The simulations using the GROMOS 43A1 force field generated multimodal distributions. The peaks with larger RMSD_{Ca} usually corresponded to conformations with partially unfolded β-sheet structures. The major difference between the two simulations was the distribution ~0.2 nm, which corresponded to conformations in the first cluster. This result was consistent with the above analysis.

The distributions of the instantaneous all heavy atom RMSD values in the simulations were plotted in **Fig. 3(B)** and with relatively large RMSDs.

Thermodynamics character of the α-syn12 peptide

To analyze the thermodynamics quantitatively in the two simulations, the stability of the unfolded state of the peptide was calculated (relative to that of the α-helix, the unfolded β-turn, and the fully folded β-hairpin structure). All the conformations of the α-syn12 peptide were divided into four different states: (i) the α-helix state (defined as helix), which comprises configurations including any helical content; (ii) the unfolded β-turn state (defined as turn), which comprises all configurations in which the K6–G7–A8–S9 turn is formed and the distance between F4(H) and A11(O) is $\geq$0.3 nm; (iii) the fully folded β-hairpin state (defined as hairpin); in this state not only the turn is formed, but also the termini are close together in space, for example, the distance between F4(H) and A11(O) is $<$0.3 nm; and (iv) the unfolded state (defined as unfolded). The relative free energy (F) can be easily obtained by the following equation:

$$\Delta F\text{State 1} \rightarrow \text{State 2} = F\text{State 2} - F\text{State 1} = -RT\ \ln(P\text{State 2}/P\text{State 1})$$

where R is the ideal gas constant, T is the temperature, and $P_{\text{State 1}}$ and $P_{\text{State 2}}$ are the probabilities in States 1 and 2, respectively.

The free energy changes from the unfolded to the helix, the unfolded to the turn, and the unfolded to the hairpin were 2.1 ± 0.6, -2.5 ± 0.6, and -1.6 ± 0.6 kJ mole^{-1}, respectively (to estimate statistical errors, the total 100 ns trajectory set was evenly divided into two 50 ns blocks for the two simulations, and the standard deviation between averages over individual blocks was computed). The -1.6 ± 0.6 kJ mole^{-1} value of $\Delta F\text{Unfolded} \rightarrow \text{Hairpin}$ can be compared with experiment for various β-peptides ranging from ~ -7 to 3 kJ mole^{-1} [52]. For H1 peptide (residues 109–122 of the Syrian hamster prion protein), the values of $\Delta F\text{Unfolded} \rightarrow \text{Hairpin}$ were 3.5 ± 0.5 kJ mole^{-1} from conventional MD simulation with the GROMOS96 force field [24] and 2.0 ± 0.5 kJ mole^{-1} from T-REMD with the GROMOS 43A1 force field [28]. These results were consistent with other amyloid disease proteins (for example, amyloid-beta peptide and H1 peptide). The results of the simulations on H1 and α-syn12 peptides

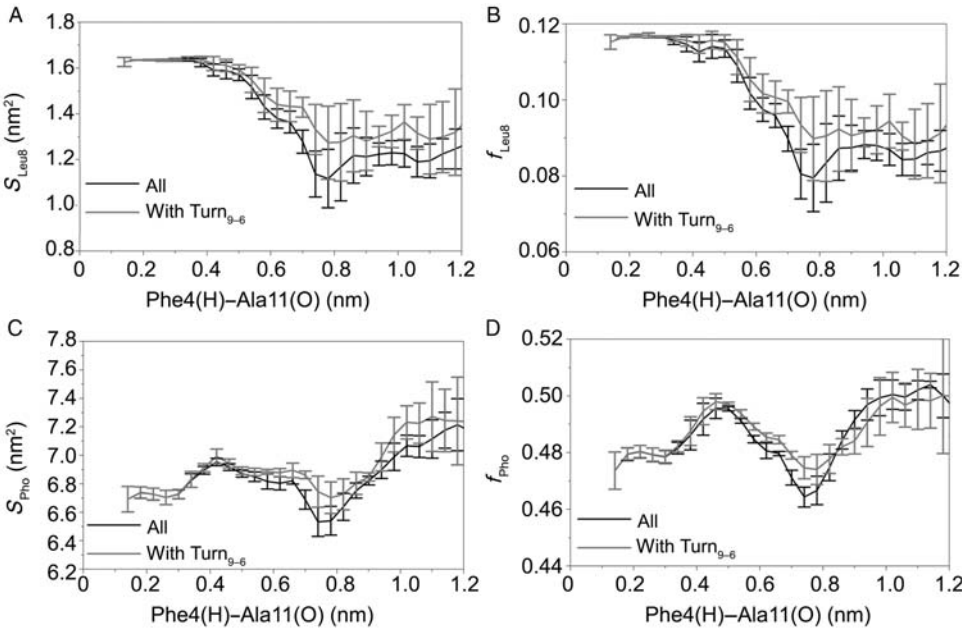

Figure 4 Solvent exposure as a function of hydrogen bond distance between Phe4(H) and Ala11(O) (A) Solvent exposure of leucine (Leu8) in the turn region, S_{Leu8}. (B) Fraction of the solvent-accessible surface that is S_{Leu8}, f_{Leu8}. (C) Solvent exposure of hydrophobic residues (Met1, Val3, Phe4, Met5, Leu8, and Ala11), S_{Pho}. (D) Fraction of the solvent-accessible surface that is S_{Pho}, f_{Pho}. Error bars correspond to a standard deviation of the corresponding property as obtained by considering four subsets of the two simulations. The black line corresponds to the analysis results from all conformations. The gray line corresponds to the analysis results only from the conformation with Turn$_{9-6}$.

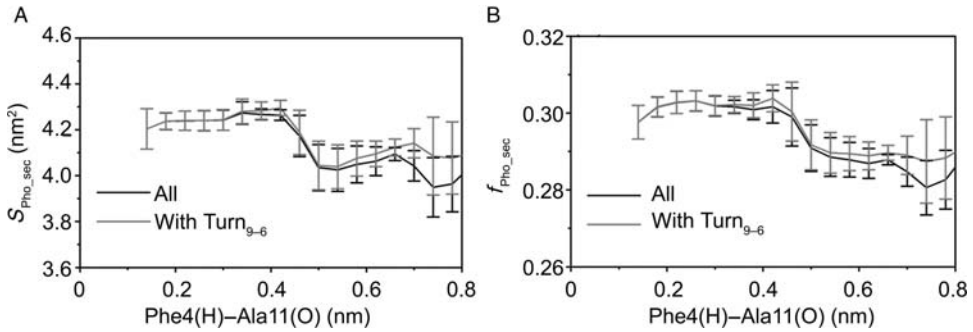

Figure 5 Solvent exposure as a function of hydrogen bond distance between Phe4(H) and Ala11(O) (A) Solvent exposure of hydrophobic residues in secondary structure (Phe4, Met5, Leu8, and Ala11), S_{Pho_sec}. (B) Fraction of the solvent-accessible surface that is S_{Pho_sec}, f_{Pho_sec}. Error bars correspond to a standard deviation of the corresponding property as obtained by considering four subsets of the two simulations. The black line corresponds to the analysis results from all conformations. The gray line corresponds to the analysis results only from the conformation with Turn$_{9-6}$.

indicated that the unfolded turn state has higher stability than the helix and the hairpin state.

Solvent exposure of hydrophobic residues in the α-syn12 peptide

To further describe the structural character of α-syn12 in solution and explore the driving force in peptide conformation transition, we calculated the solvent exposure of leucine (Leu8) in the turn region and hydrophobic residues (Met1, Val3, Phe4, Met5, Leu8, and Ala11) as a function of the distance between Phe4(H) and Ala11(O), respectively (**Fig. 4**). S_{Leu8} corresponded to the solvent exposure of leucine in the turn region; S_{Pho} corresponded to the solvent exposure of all hydrophobic residues; f_{Leu8} corresponded to the fraction of the solvent-accessible surface that is S_{Leu8}; f_{Pho} corresponded to the fraction of the solvent-accessible surface that is S_{Pho}. The analysis results were obtained from all conformations (black line) and only from the conformation with Turn$_{9-6}$ (gray line). The 100 ns trajectory of each simulation was divided into two 50 ns blocks, and the four subsets of 50 ns blocks were obtained from the two simulations. From the four subsets of blocks, the error bars were calculated based on a standard deviation of the corresponding property. The fully extended hairpin state (<0.3 nm) is characterized by high solvent exposure of the Leu8 [S_{Leu8} plotted in **Fig. 4(A)**] and low solvent exposure of the hydrophobic residues [S_{Pho} plotted in **Fig. 4(C)**]. Another instructive parameter

differentiating the folded and unfolded structures is the fraction of S_{Leu8} and S_{Pho} to the total solvent-accessible surface area (f_{Leu8} and f_{Pho}), and based on the parameter the above same results were obtained. It is possible that the high solvent exposure of hydrophobic Leu8 drives the formation of $Turn_{9-6}$. High f_{Pho} was observed for conformations with distances between 0.44 and 0.52 nm. The structures populating the distance at 0.44–0.52 nm mostly have a β-hairpin structure with two turns ($Turn_{9-6}$ and $Turn_{5-2}$) and three hydrogen bonds (HB_{6-9}, HB_{9-6}, and HB_{11-4}). These structures corresponded to the local minima B in **Fig. 2**.

To eliminate the influence of the N-terminal three residues that are not included in the secondary structure in the calculation of the solvent exposure of hydrophobic residues, the solvent exposure of hydrophobic residues in the secondary structure (Phe4, Met5, Leu8, and Ala11) as a function of the distance between Phe4(H) and Ala11(O) was calculated (**Fig. 5**). S_{Pho_sec} corresponded to the solvent exposure of hydrophobic residues in the secondary structure; f_{Pho_sec} corresponded to the fraction of solvent-accessible surface that is S_{Pho_sec}. The fully extended hairpin state (<0.3 nm) was characterized by high solvent exposure of the hydrophobic residues in the secondary structure. The high solvent exposure of Leu8 and hydrophobic residues in the secondary structure was the driving force in the peptide conformation transition.

Discussion

The mechanism and driving force in the α-syn12 peptide conformation transition can help us know the causes of Parkinson's disease. In the present work, we studied the structural and thermodynamics characters of the α-syn12 peptide in aqueous solution at atomic resolution by T-REMD simulations with the GROMOS 43A1 force field. The optimal combination of force field and water model is essential to increase MD simulation quality for different types of proteins and peptides. In recent years, many studies have been conducted to estimate which force field was the best one for protein dynamics. Takao *et al*. [53] presented the secondary structural characters with six commonly used force fields for two peptides (an α-helical polypeptide and a β-hairpin polypeptide). The results indicated that the β-hairpin is favored for the GROMOS96 43A1 force field. Rueda *et al*. [54] suggested that there was an apparent consensus view of protein dynamics using selected variants of the AMBER, CHARMM, OPLS-AA, and GROMOS96 force fields. Matthes *et al*. [55] presented a systematic study directed toward the secondary structure propensity in peptide folding simulations with eight different MD force-field variants (GROMOS96 43A1, GROMOS96 53A6, OPLS-AA/L, AMBER03, and AMBER99SB with different treatment for electrostatic interactions) in explicit solvent for five model peptides (two β-hairpins, two α-helical peptides, and trp-cage). The results indicated that AMBER03 had a slight preference for helix, the GROMOS96 43A1 force field was well balanced for most of the model peptides, and the GROMOS96 53A6 force field was highly unstable for all helical model peptides. It is difficult to estimate which is the best force field for the α-syn12 peptide without experimental information. Moreover, our recent studies [28] and the work of Daidone *et al*. [23,24] indicated that the GROMOS 43A1 force field with the SPC water model could provide more accurate results for the H1 peptide, which exhibited large solvent exposure of the hydrophobic residues. Based on the research mentioned above, the GROMOS 43A1 force field and the SPC water model were selected in this study.

The free energy surfaces and conformation clusters showed that the isolated α-syn12 peptide in solution adopted four different conformational states: the first state corresponded to the β-hairpin ensemble with $Turn_{9-6}$ and four hydrogen bonds, the second state was a β-hairpin ensemble with two turns ($Turn_{9-6}$ and $Turn_{5-2}$) and three hydrogen bonds, the third state was a disordered structure with both $Turn_{8-5}$ and $Turn_{5-2}$, and the last state was a π-helix ensemble. The free energy change of the α-syn12 peptide from the unfolded state to the hairpin state was in good agreement with the experiments and MD simulation results on some other β-peptides. The fully extended hairpin state (<0.3 nm) was characterized by high solvent exposure of Leu8 and the hydrophobic residues in the secondary structure. To the best of our knowledge, this is the first report to study the isolated α-syn12 peptide in water by T-REMD.

Acknowledgement

We would like to thank Prof. H.J.C. Berendsen (University of Groningen) for providing us with the GROMACS programs.

Funding

This work was supported by grants from the National Natural Science Foundation of China (30970561 and 31000324) and the Shandong Province Natural Science Foundation (2009ZRA14027 and 2009ZRA14028).

References

1 Soto C. Alzheimer's and prion disease as disorders of protein conformation: implications for the design of novel therapeutic approaches. J Mol Med 1999, 77: 412–418.

2 Zanusso G, Farinazzo A, Fiorini M, Gelati M, Castagna A, Righetti PG and Rizzuto N, *et al*. pH-dependent prion protein conformation in classical Creutzfeldt–Jakob disease. J Biol Chem 2001, 276: 40377–40380.
3 Harrison RS, Sharpe PC, Singh Y and Fairlie DP. Amyloid peptides and proteins in review. Rev Physiol Biochem Pharmacol 2007, 159: 1–77.
4 Ollesch J, Kunnemann E, Glockshuber R and Gerwert K. Prion protein alpha-to-beta transition monitored by time-resolved Fourier transform infrared spectroscopy. Appl Spectrosc 2007, 61: 1025–1031.
5 Malolepsza EB. Modeling of protein misfolding in disease. Methods Mol Biol 2008, 443: 297–330.
6 Surguchev A and Surguchov A. Conformational diseases: looking into the eyes. Brain Res Bull 2009, 81: 12–24.
7 Bharadwaj PR, Dubey AK, Masters CL, Martins RN and Macreadie IG. Abeta aggregation and possible implications in Alzheimer's disease pathogenesis. J Cell Mol Med 2009, 13: 412–421.
8 Murphy MP and Levine H, III. Alzheimer's disease and the amyloid-beta peptide. J Alzheimers Dis 2010, 19: 311–323.
9 Subramanian S, Madhavadas S and Balasubramanian P. Influence of conformational antibodies on dissociation of fibrillar amyloid beta (A beta 1–42) *in vitro*. Indian J Exp Biol 2009, 47: 309–313.
10 Cobb NJ and Surewicz WK. Prion diseases and their biochemical mechanisms. Biochemistry 2009, 48: 2574–2585.
11 Kupfer L, Hinrichs W and Groschup MH. Prion protein misfolding. Curr Mol Med 2009, 9: 826–835.
12 Lees AJ, Hardy J and Revesz T. Parkinson's disease. Lancet 2009, 373: 2055–2066.
13 Pankratz N, Nichols WC, Elsaesser VE, Pauciulo MW, Marek DK, Halter CA and Wojcieszek J, *et al*. Alpha-synuclein and familial Parkinson's disease. Mov Disord 2009, 24: 1125–1131.
14 Schapira AH. Etiology and pathogenesis of Parkinson disease. Neurol Clin 2009, 27: 583–603.
15 Yang YX, Wood NW and Latchman DS. Molecular basis of Parkinson's disease. Neuroreport 2009, 20: 150–156.
16 Yu J and Lyubchenko YL. Early stages for Parkinson's development: alpha-synuclein misfolding and aggregation. J Neuroimmune Pharmacol 2009, 4: 10–16.
17 Bisaglia M, Mammi S and Bubacco L. Structural insights on physiological functions and pathological effects of alpha-synuclein. FASEB J 2009, 23: 329–340.
18 Ulmer TS, Bax A, Cole NB and Nussbaum RL. Structure and dynamics of micelle-bound human alpha-synuclein. J Biol Chem 2005, 280: 9595–9603.
19 Georgieva ER, Ramlall TF, Borbat PP, Freed JH and Eliezer D. Membrane-bound alpha-synuclein forms an extended helix: long-distance pulsed ESR measurements using vesicles, bicelles, and rodlike micelles. J Am Chem Soc 2008, 130: 12856–12857.
20 Engelender S, Kaminsky Z, Guo X, Sharp AH, Amaravi RK, Kleiderlein JJ and Margolis RL, *et al*. Synphilin-1 associates with alpha-synuclein and promotes the formation of cytosolic inclusions. Nat Genet 1999, 22: 110–114.
21 Xie YY, Zhou CJ, Zhou ZR, Hong J, Che MX, Fu QS and Song AX, *et al*. Interaction with synphilin-1 promotes inclusion formation of alpha-synuclein: mechanistic insights and pathological implication. FASEB J 2009, 24: 196–205.
22 Daidone I, Simona F, Roccatano D, Broglia RA, Tiana G, Colombo G and Di Nola A. Beta-hairpin conformation of fibrillogenic peptides: structure and alpha-beta transition mechanism revealed by molecular dynamics simulations. Proteins 2004, 57: 198–204.
23 Daidone I, Amadei A and Di Nola A. Thermodynamic and kinetic characterization of a beta-hairpin peptide in solution: an extended phase space sampling by molecular dynamics simulations in explicit water. Proteins 2005, 59: 510–518.
24 Daidone I, Ulmschneider MB, Di Nola A, Amadei A and Smith JC. Dehydration-driven solvent exposure of hydrophobic surfaces as a driving force in peptide folding. Proc Natl Acad Sci USA 2007, 104: 15230–15235.
25 Chiang YW, Otoshima Y, Watanabe Y, Inanami O and Shimoyama Y. Dynamics and local ordering of spin-labeled prion protein: an ESR simulation study of a highly PH-sensitive site. J Biomol Struct Dyn 2008, 26: 355–366.
26 Levy Y, Hanan E, Solomon B and Becker OM. Helix–coil transition of PrP106–126: molecular dynamic study. Proteins 2001, 45: 382–396.
27 Klimov DK and Thirumalai D. Dissecting the assembly of Abeta16–22 amyloid peptides into antiparallel beta sheets. Structure 2003, 11: 295–307.
28 Cao ZX and Wang JH. A comparative study of two different force fields on structural and thermodynamics character of H1 peptide via molecular dynamics simulations. J Biomol Struct Dyn 2010, 27: 651–661.
29 Sugita Y and Okamoto Y. Replica-exchange molecular dynamics method for protein folding. Chem Phys Lett 1999, 314: 141–151.
30 Zhou R, Berne BJ and Germain R. The free energy landscape for beta hairpin folding in explicit water. Proc Natl Acad Sci USA 2001, 98: 14931–14936.
31 Suzuki M and Okuda H. Fragment replica-exchange method for efficient protein conformation sampling. Mol Simul 2008, 34: 267–275.
32 Yoon J, Park J, Jang S, Lee K and Shin S. Conformational characteristics of unstructured peptides: alpha-synuclein. J Biomol Struct Dyn 2008, 25: 505–515.
33 Kawashima Y, Sasaki YC, Sugita Y, Yoda T and Okamoto Y. Replica-exchange molecular dynamics simulation of diffracted X-ray tracking. Mol Simul 2007, 33: 97–102.
34 Periole X and Mark AE. Convergence and sampling efficiency in replica exchange simulations of peptide folding in explicit solvent. J Chem Phys 2007, 126: 014903.
35 Zhang J, Qin M and Wang W. Folding mechanism of beta-hairpins studied by replica exchange molecular simulations. Proteins 2006, 62: 672–685.
36 Zhou R and Berne BJ. Can a continuum solvent model reproduce the free energy landscape of a beta-hairpin folding in water? Proc Natl Acad Sci USA 2002, 99: 12777–12782.
37 Nguyen PH, Stock G, Mittag E, Hu CK and Li MS. Free energy landscape and folding mechanism of a beta-hairpin in explicit water: a replica exchange molecular dynamics study. Proteins 2005, 61: 795–808.
38 Dinner AR, Lazaridis T and Karplus M. Understanding beta-hairpin formation. Proc Natl Acad Sci USA 1999, 96: 9068–9073.
39 Garcia AE and Sanbonmatsu KY. Exploring the energy landscape of a beta hairpin in explicit solvent. Proteins 2001, 42: 345–354.
40 Van Der Spoel D, Lindahl E, Hess B, Groenhof G, Mark AE and Berendsen HJC. GROMACS: fast, flexible, and free. J Comput Chem 2005, 26: 1701.
41 van Gunsteren WF, Billeter SR, Eising AA, Hünenberger PH, Krüger P, Mark AE and Scott WRP, *et al*. Biomolecular Simulation: The GROMOS96 Manual and User Guide. Switzerland: Vdf Hochschulverlag AG an der ETH Zürich, 1996, 1.
42 Berendsen HJC, Postma JPM, van Gunsteren WF and Hermans J. Interaction models for water in relation to protein hydration. In: Pullman B ed. Intermolecular Forces. Dordrecht: Reidel, 1981, 331.
43 Tironi IG, Sperb R, Smith PE and van Gunsteren WF. A generalized reaction field method for molecular dynamics simulations. J Chem Phys 1995, 102: 5451.
44 Berendsen HJC, Postma JPM, van Gunsteren WF, DiNola A and Haak JR. Molecular dynamics with coupling to an external bath. J Chem Phys 1984, 81: 3684.
45 Ryckaert J-P, Ciccotti G and Berendsen HJC. Numerical integration of the Cartesian equations of motion of a system with constraints: molecular dynamics of *n*-alkanes. J Comput Phys 1977, 23: 327.
46 Patriksson A and van der Spoel D. A temperature predictor for parallel tempering simulations. Phys Chem Chem Phys 2008, 10: 2073–2077.

47 Hu H, Elstner M and Hermans J. Comparison of a QM/MM force field and molecular mechanics force fields in simulations of alanine and glycine "dipeptides" (Ace-Ala-Nme and Ace-Gly-Nme) in water in relation to the problem of modeling the unfolded peptide backbone in solution. Proteins 2003, 50: 451–463.
48 Heinig M and Frishman D. STRIDE: a web server for secondary structure assignment from known atomic coordinates of proteins. Nucleic Acids Res 2004, 32(Web Server issue): W500–W502.
49 Frishman D and Argos P. Knowledge-based protein secondary structure assignment. Proteins 1995, 23: 566–579.
50 Maria MA. Biophysical Studies of the alpha-Synuclein Protein Associated with Parkinson's Disease and Other Synucleinopathies. Ohio: Case Western Reserve University, 2006.
51 Garcia AE. Large-amplitude nonlinear motions in proteins. Phys Rev Lett 1992, 68: 2696–2699.
52 Munoz V, Ghirlando R, Blanco FJ, Jas GS, Hofrichter J and Eaton WA. Folding and aggregation kinetics of a beta-hairpin. Biochemistry 2006, 45: 7023–7035.
53 Takao Y, Yuji S and Yuko O. Comparisons of force fields for proteins by generalized-ensemble simulations. Chem Phys Lett 2004, 386: 460–467.
54 Rueda M, Ferrer-Costa C, Meyer T, Perez A, Camps J, Hospital A and Gelpi JL, *et al*. A consensus view of protein dynamics. Proc Natl Acad Sci USA 2007, 104: 796–801.
55 Matthes D and de Groot BL. Secondary structure propensities in peptide folding simulations: a systematic comparison of molecular mechanics interaction schemes. Biophys J 2009, 97: 599–608.